analytical chemistry

pubs.acs.org/ac

Technical Note

Tunable and Contamination-Free Injection with Microfluidics by Stepinjection

Beiyu Hu, Shun Ye, Dongwei Chen, Bingliang Xie, Ran Hu, Yuxin Qiao, Yanghuan Yu, Haiyan Yu, Xu Zheng, Ying Lan, and Wenbin Du*

Cite This: *Anal. Chem.* 2021, 93, 13112–13117

Read Online

ACCESS | Metrics & More | Article Recommendations | Supporting Information

ABSTRACT: Droplet microfluidics with picoinjection provides significant advantages to multistep reactions and screenings. The T-junction design for picoinjection is convenient in adding picoliter reagents into passing droplets to initiate reactions. However, conventional picoinjectors face difficulties in eliminating cross-contamination between droplets, preventing them from widespread use in sensitive biological and molecular assays. Here, we introduce stepinjection, which uses a T-junction with a stepped channel design to elevate the diffusional buffer zone into the main channel and consequently increases the pressure difference between droplets and the inlet of the injection channel. To demonstrate the stepinjector's ability to perform contamination-sensitive enzymatic assays, we inject casein fluorescein isothiocyanate (FITC-casein) into a mixture of savinase and savinase-free (labeled with a red fluorescent dye) droplets. We observe no cross-contamination using stepinjection but find a severe cross-talk using an optimal picoinjection design. We envision that the simple, tunable, and reliable stepinjector can be easily integrated in various droplet processing devices, and facilitate various biomedical and biochemical applications including multiplex digital PCR, single-cell sequencing, and enzymatic screening.

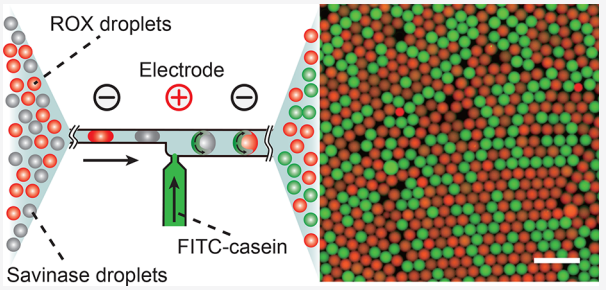

INTRODUCTION

Droplet microfluidics is a powerful technique employed for a myriad of biological applications (e.g., cell culture, enzymatic assay, antimicrobial susceptibility testing, and molecular diagnosis).[1−3] Compared to conventional bulk experiments performed using flasks or multiple-well plates, high-throughput biochemical assays using droplet-based microreactors offer numerous inherent advantages, such as low sample consumption and large scale parallelization.[4,5] For a majority of droplet-based multistep biological reactions, however, adding reagents into droplets in an optimal predefined condition after droplets generation is highly desired. For dosing reagents into droplets, picoinjection is developed to directly inject reagents from a side channel into droplets with the aid of an electric field;[6,7] droplet coalescence is established to pair and merge two droplets of different components and volumes.[8,9] In comparison, picoinjection is feasible, flexible, and controllable to add reagents into droplets, with variable volumes, ruling out the complexity and instability of drop pairing and coalescence. Given the above features, picoinjection has been applied in multistep enzymatic assays,[10] single-cell sequencing,[11] loop-mediated isothermal amplification (LAMP),[12] and cell−cell interaction assays.[13]

Unfortunately, a technical barrier that hinders the prevalence of picoinjection is the cross-contamination between droplets.[14] In detail, when adding the substrate into droplets with a conventional picoinjector, the reagent in the droplet is immediately merged with the substrate at the orifice of the side channel. This allows the reagent in the droplet to diffuse into the side channel and contaminate the substrate at the orifice during picoinjection. The residual reagent left by the former droplet would be injected into the subsequent droplet, resulting in cross-contamination between droplets (Figure 1a). Such contamination severely limits the picoinjector's usability and reduces the reliability of experimental results in many sensitive biological and biocatalytic assays. For example, single-cell sequencing by using droplet-based barcoding would fail due to the cross-contamination during injecting cells or nucleic acid amplification reagents into barcode droplets.[15] Besides, injecting fluorogenic substrate into an array of enzyme-containing droplets for high-throughput enzyme screening would yield a low efficiency due to increased false-positive droplets after cross-contamination.[16]

Although the risk of interdroplet cross-contamination of picoinjection persists, only a few studies discussed its adverse

Received: June 29, 2021
Published: September 21, 2021

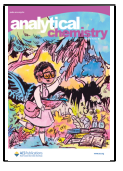

https://doi.org/10.1021/acs.analchem.1c02721
Anal. Chem. 2021, 93, 13112−13117

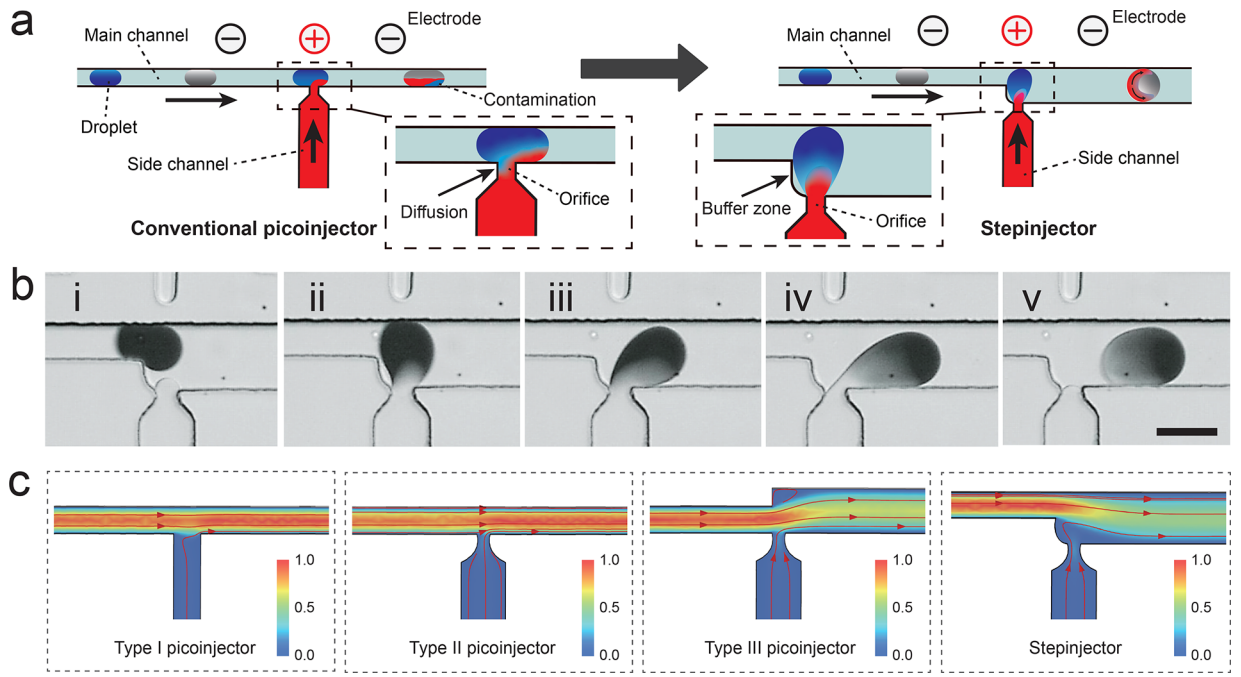

Figure 1. Design and working principle of stepinjection. (a) A schematic illustrates the difference between conventional picoinjector (*left*) and stepinjector (*right*) during substrate injection. (b) The time-lapse images taken by a high-speed video camera showing the picoinjection process for injecting deionized water into a blue food dye droplet using stepinjector. Scale bar is 50 μm. (c) The COMSOL simulation of the fluid velocity distribution and streamline of type I, type II, type III picoinjectors, and stepinjector.

influence. The cross-contamination between droplets during picoinjection was first reported by conducting multiplex droplet reverse trascription PCR (RT-PCR).[14] Afterward, several studies made an effort to reduce such cross-contamination, one attempt was to insert a quartz capillary into the side channel,[17] and an alternative method was to introduce a "K-channel" design to wash away residual reagents.[18] However, to the best of our knowledge, few existing picoinjection designs demonstrate contamination-free substrate injection, especially for enzymatic reactions and nucleic acids amplification testings. Thus, a contamination-free picoinjector for highly sensitive enzymatic/molecular assays is highly desired. Herein, we developed stepinjection, a novel microfluidic method possessing a T-junction with a stepped channel design, for injecting reagents into droplets without cross-contamination. The performance of three widely adopted picoinjectors and a stepinjector were investigated and compared. We successfully achieved contamination-free reagent picoliter injection spanning a wide volume range using the stepinjector. As a proof-of-concept, a contamination-sensitive enzymatic assay was performed in order to validate the feasibility of injecting reagents into droplets without cross-contamination using the stepinjector. The simple, feasible, contamination-free stepinjector has great potential for various biological and clinical applications such as single-cell analysis and precision molecular diagnosis.

EXPERIMENTAL SECTION

Fabrication and Operation of Microfluidic Devices. The microfluidic devices were fabricated in Poly(dimethylsiloxane) (PDMS) using standard soft lithography with SU-8 photoresist (Microchem, USA).[19,20] Fluorinated oil (Droplet Generation Oil for EvaGreen, Bio-Rad, USA) was used as a continuous phase for droplet generation and picoinjection. A high-voltage amplifier (TREK, USA) was used to generate an electric field to induce droplet merging. The injected volume was quantified by measuring droplet radii before and after picoinjection. All images were analyzed using ImageJ software (NIH, USA) unless otherwise mentioned. The fluid simulations were performed using COMSOL Multiphysics (COMSOL Inc., USA). Detailed experimental procedures were described in the Supporting Information (Text S1).

RESULTS AND DISCUSSION

Design and Verification of Stepinjector. To investigate the determining factors of the cross-contamination during picoinjection, we fabricated three types of picoinjectors as previously reported.[6,11,14,21] Figure S1 shows the time-lapse images of the picoinjection process using type I (Figure S1b), type II (Figure S1c), and type III (Figure S1d) picoinjectors, recorded by a high-speed video camera. During injection of deionized water (substrate) into blue food dye droplets, all three types of picoinjection devices suffered from cross-contamination (Figure S1). To tackle this key issue, we introduced the modified picoinjector we termed as stepinjector, which adopted the two features as previously reported (i.e., narrowed side channel and widened main channel). More importantly, in the optimized stepinjector design we move the stepped structure to the location between the serially passing droplet and the orifice of the side channel, in contrast to the type III picoinjector where the stepped structure was set in the opposite position (the optimization process of the stepinjector is described in the Supporting Information (SI) and Figure S2). This stepped structure provides more space for the merging of the droplet and the substrate flowing out of the side channel, thus elevating the diffusional buffer zone of the droplet farther from the orifice (Figure 1a *right* and 1b). For conventional picoinjectors as demonstrated in Figure 1a *left*, the diffusional zone of the droplet was located just in the orifice of the side channel, contaminating the substrate as the

https://doi.org/10.1021/acs.analchem.1c02721
Anal. Chem. 2021, 93, 13112−13117

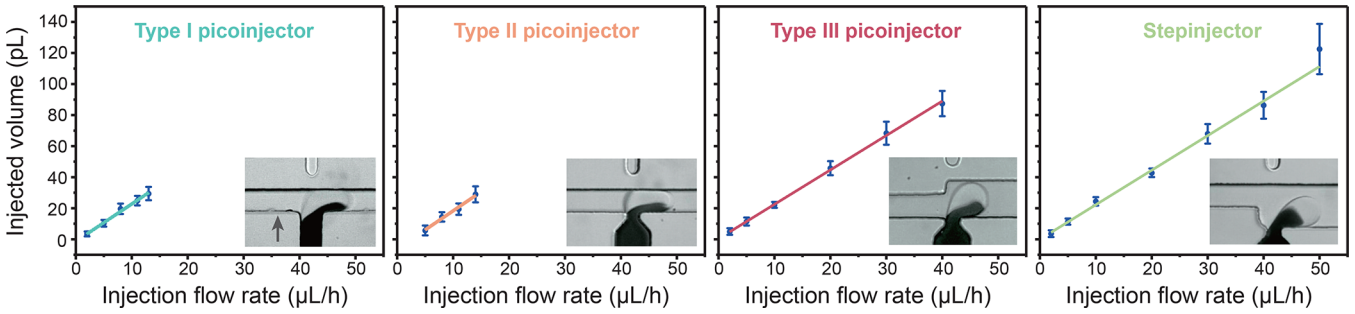

Figure 2. Range of injection volume for picoinjectors and the stepinjector. The volume of the injected substrate can be increased by raising the flow rate of the substrate. Stepinjector demonstrates a wider injection range, compared to the other three types of picoinjectors.

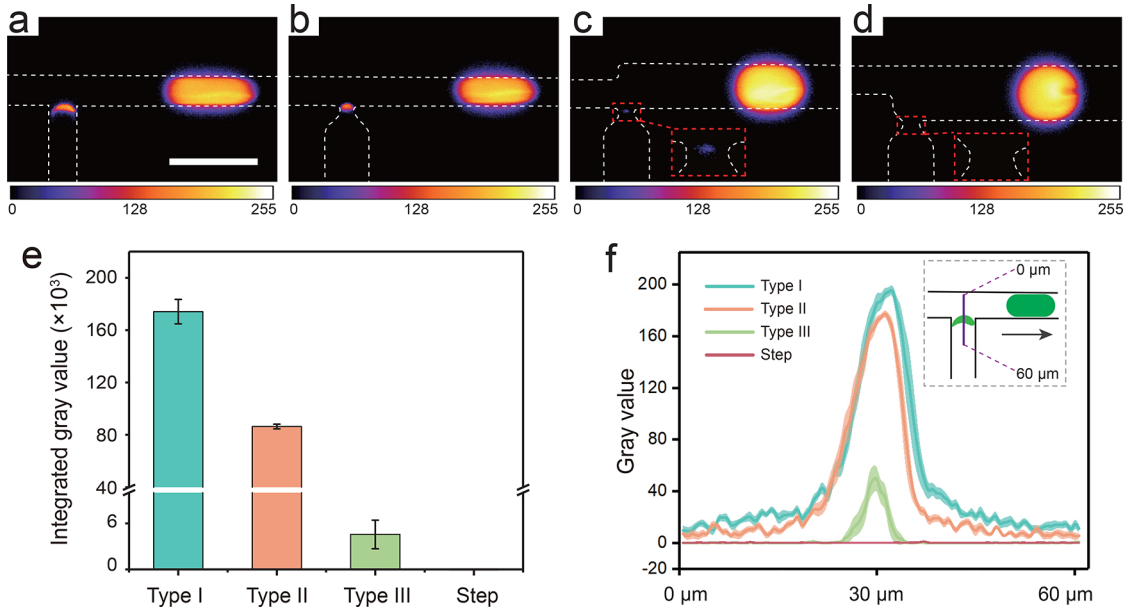

Figure 3. Evaluation of cross-contamination for four types of injectors. (a–d) Fluorescence images demonstrate the intensity distribution of the residual fluorescein at the orifice of type I, type II, type III picoinjectors, and the stepinjector. Scale bar is 100 μm. (e) The integrated gray value of residual fluorescein at the orifice of the four types of injectors. (f) The intensity profiles of the center-line across the side channel of the four types of picoinjectors. The peak values shown in the profiles represent the max gray value of residual fluorescein at the orifice of the side channel.

residue diffuses into the side channel. Figure 1a *right* demonstrates that the diffusional zone of the droplet is shifted to the main channel out of the orifice, delimiting the diffusion of content in the main channel and reducing the possibility of contamination (see Text S2 for details in the Supporting Information).

To explain the design principle of stepinjection, we divide the injection process into the following phases (Figure 1b): (i) the droplet is approaching the injection zone, and the substrate bulges into the buffer zone (Figure 1b(i)); (ii) the coalescence of the droplet and substrate triggered by an electric field (Figure 1b(ii)); (iii) the substrate is injected into the droplet, and the diffusion occurs in the buffer zone instead of the orifice of the side channel (Figure 1b(iii)); (iv) the bridge between droplet and substrate narrows and breaks, eventually completing the injection process (Figure 1b(iv)–(v)). We performed flow simulations for different picoinjectors using COMSOL software in order to evaluate the cross-contamination during injection. The fluid velocity distribution and streamline simulation results of four picoinjectors are shown in Figure 1c. The results showed that the normalized fluid velocities near the orifice of the side channel of type I, II, and III picoinjectors were considerably higher than that of the stepinjector (Figure 1c). Particularly for the stepinjector, the fast flow (represented as red area) mainly "pushes" the top region of the droplet, generating a clockwise torque that facilitates the break-off of the bridge between the droplet and the substrate. This effect significantly reduces the possibility of the diffusional transport of the residue into the orifice of the side channel. The flow simulation results match well with the experimental observation, as shown in Movie S1.

Characterization of the Stepinjector. One of the important characteristics of the picoinjector is ease of controlling the volume of the injected substrate by adjusting parameters, such as the flow velocities of the emulsion and substrate. To verify the feasibility of controllable substrate injection using our stepinjector, we quantified the volume of the injected substrate by measuring the radii of the droplet before and after picoinjection. We first set the voltage applied to the electrodes, the flow velocities of the emulsion, and the spacing oil as constants and increased the flow velocities of the substrate to compare the injected volume range of the picoinjectors and the stepinjector (Figure 2). The results showed that as the flow rate of the substrate increased, the volume of the injected substrate also increased from 3.5 to 122 pL for the stepinjector, and type III picoinjector also

https://doi.org/10.1021/acs.analchem.1c02721
Anal. Chem. 2021, 93, 13112–13117

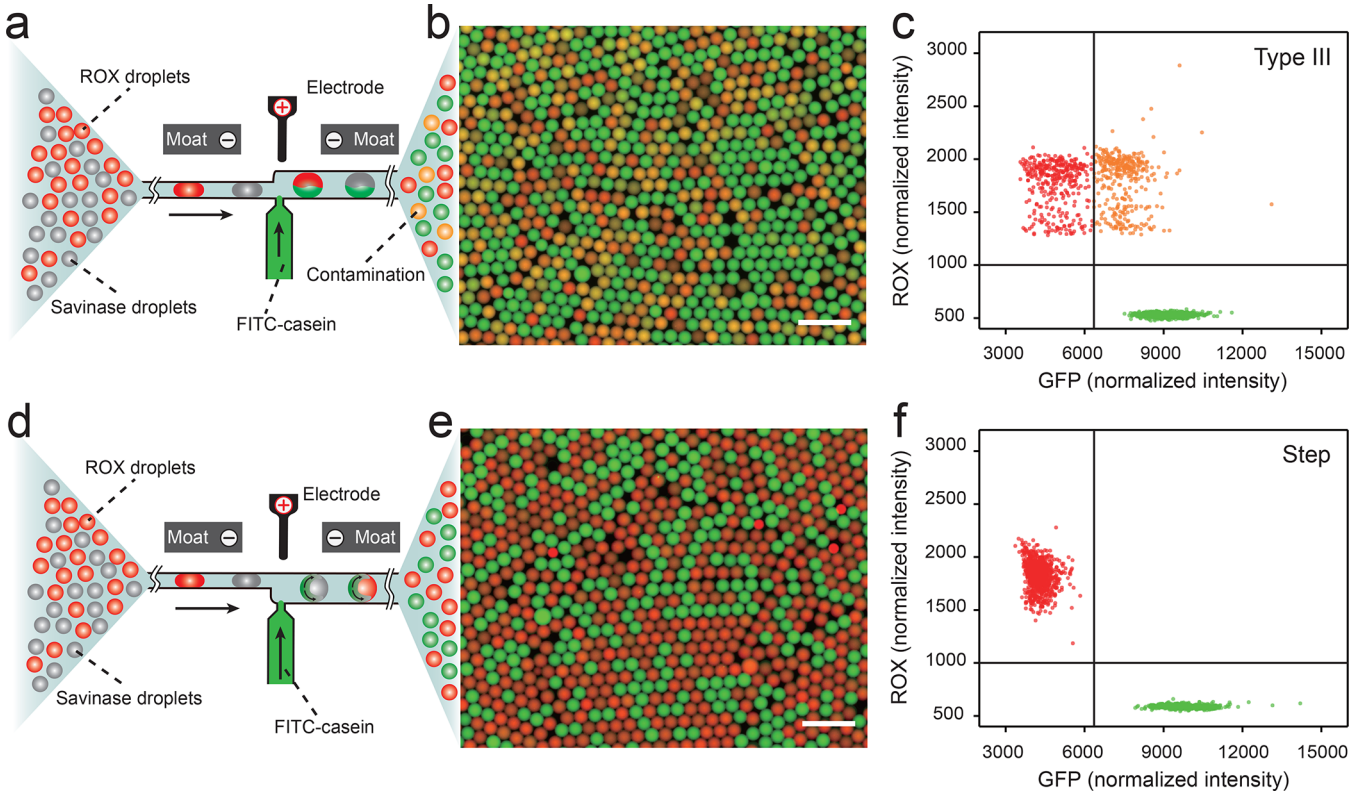

Figure 4. Enzymatic assays for the comparison between type III picoinjector and the stepinjector. (a and d) Schematics show the process of adding the fluorogenic substrate into positive droplets of savinase and negative droplets of ROX for enzymatic analysis, which is performed using type III picoinjector and stepinjector, respectively. (b and e) The fluorescence images of droplets after substrate injection and 20 min incubation. Green and red droplets only contain savinase and ROX, respectively. Yellow droplets indicate contamination by residual savinase during injection. Scale bar is 200 μm. (c and f) Scatter plots of the fluorescent intensity distribution of droplets of type III picoinjector and stepinjector.

demonstrated a wide volume range (4.9−87 pL), whereas the injected substrate volume ranges of the type I and II picoinjectors were 5.6−28.9 pL and 3.4−29 pL, respectively. Moreover, we set the flow rate of the substrate as a constant, increasing the flow rate of the emulsion which increases the frequency of droplets passing through the picoinjector, resulting in a sequential decrease in the volume of the injected substrate (Figure S3a). Besides, the injection volume ratio (specified as the volume of injected substrate divided by the original volume of the droplet) of our stepinjector was higher than the other three types of picoinjectors due to the widened main channel and the diffusional buffer zone (Figure S3b). A high injection ratio would be a appealing trait in droplet chemostats, and the multijunction injection device was also developed to increase the injection ratio of the nanoliter droplet as demonstrated by previous reports.[22,23] However, it would be difficult to design a multijunction injection device with a high injection ratio for picoliter droplets, because the size limitation of microfabrication. In contrast, the stepinjector is a simple and reliable approach to achieve a high injection ratio for picoinjection.

Characterization of the Cross-Contamination of Different Picoinjectors. We further quantified the cross-contamination of four picoinjectors using the fluorescein solution as the emulsion and deionized water as injection substrate. Before picoinjection, we adopted light shielding methods to reduce fluorescein quenching, as described in the Supporting Information (Text S1, Text S3, and Figure S4). As shown in Figure S1b−d, residual reagents (food dye) can be observed at the orifice of the side channel after picoinjection. To evaluate the amount of residual fluorescein contaminating the injectors, we captured the fluorescence images at the injection zones during picoinjection. Similar to our results shown in Figure S1, there were fluorescence residuals at the orifice of the side channels of three conventional picoinjectors, and no residuals were observed at the orifice of the stepinjector, as shown in Figure 3a−d and Movie S2. To quantify the cross-contamination between the droplets and the substrate, we calculated integrated fluorescence intensities of the orifice of the side channels, which were decreased in sequence (from type I, II, and III picoinjectors to the stepinjector) (Figure 3e), and the intensity profiles of the center-line across the side channel of four types of injectors were also recorded and plotted in Figure 3f. The integrated and maximum (peak values shown in the intensity profiles) fluorescence intensity could partially represent the volume and the concentration of the fluorescein residuals, respectively. Importantly, fluorescein residuals were undetectable using the stepinjector, indicating that stepinjection substantially eliminated the cross-contamination.

Droplet-Based Enzymatic Assays. To demonstrate stepinjector's ability for contamination-free enzymatic assays using droplet microfluidics, we performed a contamination-sensitive enzymatic reaction with savinase hydrolysis of FITC-casein. Savinase is a broad spectrum endoprotease for animal protein extraction.[24,25] We synthesized a fluorogenic substrate FITC-casein, which can emit strong green fluorescence in the GFP channel after hydrolysis catalyzed by savinase. We used FITC-casein as the injected substrate in the type III picoinjector and stepinjector to investigate cross-contamina-

https://doi.org/10.1021/acs.analchem.1c02721
Anal. Chem. 2021, 93, 13112−13117

tion between ROX (carboxy-X-rhodamine with red fluorescence in the RFP channel) and savinase droplets (Figure 4a, 4d). The ROX and savinase droplets were generated separately and mixed before being reinjected into the picoinjection devices to add FITC-casein to each droplet. After injection and 20 min incubation, we imaged the droplet array in both RFP and GFP channels, and counted the RFP-positive droplets (red, ROX droplets uncontaminated), GFP-positive droplets (green, savinase droplets after injecting FITC-casein), and double positive droplets (brown, ROX droplets contaminated by residual savinase during picoinjection). As expected, an extremely small amount of residual savinase at the orifice of the side channel from the previous droplet will contaminate the next incoming droplet, resulting in double positive cases. The results showed that the contamination ratio of type III and stepinjectors were 50% (359 RFP, 672 GFP, and 359 contaminated droplets) and 0% (867 RFP, 572 GFP, and 0 contaminated droplets), respectively (Figure 4). The results show that stepinjection minimizes contamination risk, demonstrating full accessibility for high-performance droplet-based analysis.

CONCLUSIONS

In this work, we developed stepinjection, a simple microfluidic technique for controllable dose of reagents into droplets with a wide injection volume ratio without contamination. We introduced the stepped structure in the main channel to shift the diffusional buffer zone of the droplet out of the orifice and to provide an extra space for the mixing in the droplet, which eliminates cross-contamination by suppressing the diffusional transport into the side channel. Thus, our stepinjector can perform reliable picoliter injection without cross-contamination between droplet and substrate, which cannot be achieved by existing methods (i.e., picoinjection or paired droplets coalescence devices). This stepinjector has shown high performance in droplet-based enzymatic assays, demonstrating considerable potential in the applications of droplet microfluidics. We envision that stepinjection would be a powerful tool for biological studies, including single-cell sorting,[16] single-cell sequencing,[15] enzymatic analysis,[26,27] molecular diagnosis,[12] etc.

ASSOCIATED CONTENT

Supporting Information

The Supporting Information is available free of charge at https://pubs.acs.org/doi/10.1021/acs.analchem.1c02721.

Experimental details, optimization of the microfluidic devices, analysis of cross-contamination, strategies to avoid fluorescent quenching of droplets during reinjection into the devices (PDF)

CAD designs of the picoinjection and stepinjection devices used in this study (ZIP)

Comparison of picoinjection and stepinjection of food-dye solution into deionized water droplets, recorded by a high-speed video camera (Movie S1) (AVI)

Comparison of picoinjection and stepinjection of deionized water into fluorescein droplets, recorded by a high-speed video camera (Movie S2) (AVI)

AUTHOR INFORMATION

Corresponding Author

Wenbin Du − *State Key Laboratory of Microbial Resources, Institute of Microbiology, Chinese Academy of Sciences, Beijing 100101, China; Savaid Medical School, University of the Chinese Academy of Sciences, Beijing 100049, China; State Key Laboratory of Transducer Technology, Institute of Microbiology, Chinese Academy of Sciences, Beijing 100101, China;* orcid.org/0000-0002-7401-1410; Email: wenbin@im.ac.cn

Authors

Beiyu Hu − *State Key Laboratory of Microbial Resources, Institute of Microbiology, Chinese Academy of Sciences, Beijing 100101, China; College of Life Sciences, University of the Chinese Academy of Sciences, Beijing 100049, China; State Key Laboratory of Transducer Technology, Institute of Microbiology, Chinese Academy of Sciences, Beijing 100101, China*

Shun Ye − *State Key Laboratory of Microbial Resources, Institute of Microbiology, Chinese Academy of Sciences, Beijing 100101, China; Biomedical Engineering Department, College of Engineering, Pennsylvania State University, University Park, Pennsylvania 16802, United States;* orcid.org/0000-0003-3457-9359

Dongwei Chen − *State Key Laboratory of Microbial Resources, Institute of Microbiology, Chinese Academy of Sciences, Beijing 100101, China; State Key Laboratory of Transducer Technology, Institute of Microbiology, Chinese Academy of Sciences, Beijing 100101, China;* orcid.org/0000-0002-0471-6298

Bingliang Xie − *State Key Laboratory of Microbial Resources, Institute of Microbiology, Chinese Academy of Sciences, Beijing 100101, China; College of Life Sciences, University of the Chinese Academy of Sciences, Beijing 100049, China*

Ran Hu − *State Key Laboratory of Microbial Resources, Institute of Microbiology, Chinese Academy of Sciences, Beijing 100101, China; State Key Laboratory of Transducer Technology, Institute of Microbiology, Chinese Academy of Sciences, Beijing 100101, China*

Yuxin Qiao − *State Key Laboratory of Microbial Resources, Institute of Microbiology, Chinese Academy of Sciences, Beijing 100101, China; State Key Laboratory of Transducer Technology, Institute of Microbiology, Chinese Academy of Sciences, Beijing 100101, China*

Yanghuan Yu − *State Key Laboratory of Microbial Resources, Institute of Microbiology, Chinese Academy of Sciences, Beijing 100101, China*

Haiyan Yu − *State Key Laboratory of Microbial Resources, Institute of Microbiology, Chinese Academy of Sciences, Beijing 100101, China; Savaid Medical School, University of the Chinese Academy of Sciences, Beijing 100049, China*

Xu Zheng − *State Key Laboratory of Nonlinear Mechanics, Institute of Mechanics, Chinese Academy of Sciences, Beijing 100190, China;* orcid.org/0000-0002-2398-9283

Ying Lan − *State Key Laboratory of Microbial Resources, Institute of Microbiology, Chinese Academy of Sciences, Beijing 100101, China*

Complete contact information is available at: https://pubs.acs.org/10.1021/acs.analchem.1c02721

Notes

The authors declare no competing financial interest.

■ ACKNOWLEDGMENTS

This work was supported by the National Key Research and Development Program of China (2018YFC0310703, 2016YFE0205800), International Ocean Resource Survey and Exploration (DY135-B-02), the National Natural Science Foundation of China (21822408, 91951103, 12072350, 11832017, and 32100073), the Key Program of Frontier Sciences of the Chinese Academy of Sciences (QYZDB-SSW-SMC008, QYZDB-SSW-JSC036), the CAS Strategic Priority Research Program (XDB22040403), and the Center for Ocean Mega-Science, Chinese Academy of Sciences (KEX-UE2019GZ05).

■ REFERENCES

(1) Guo, M. T.; Rotem, A.; Heyman, J. A.; Weitz, D. A. *Lab Chip* **2012**, *12*, 2146−2155.
(2) Matuła, K.; Rivello, F.; Huck, W. T. S. *Adv. Biosyst.* **2020**, *4*, 1900188.
(3) Obexer, R.; Godina, A.; Garrabou, X.; Mittl, P. R. E.; Baker, D.; Griffiths, A. D.; Hilvert, D. *Nat. Chem.* **2017**, *9*, 50−56.
(4) Kaminski, T. S.; Scheler, O.; Garstecki, P. *Lab Chip* **2016**, *16*, 2168−2187.
(5) Theberge, A. B.; Courtois, F.; Schaerli, Y.; Fischlechner, M.; Abell, C.; Hollfelder, F.; Huck, W. T. S. *Angew. Chem., Int. Ed.* **2010**, *49*, 5846−5868.
(6) Abate, A. R.; Hung, T.; Mary, P.; Agresti, J. J.; Weitz, D. A. *Proc. Natl. Acad. Sci. U. S. A.* **2010**, *107*, 19163.
(7) O'Donovan, B.; Eastburn, D. J.; Abate, A. R. *Lab Chip* **2012**, *12*, 4029−4032.
(8) Brouzes, E.; Medkova, M.; Savenelli, N.; Marran, D.; Twardowski, M.; Hutchison, J. B.; Rothberg, J. M.; Link, D. R.; Perrimon, N.; Samuels, M. L. *Proc. Natl. Acad. Sci. U. S. A.* **2009**, *106*, 14195.
(9) Kim, S. C.; Clark, I. C.; Shahi, P.; Abate, A. R. *Anal. Chem.* **2018**, *90*, 1273−1279.
(10) Ng, E. X.; Miller, M. A.; Jing, T.; Lauffenburger, D. A.; Chen, C.-H. *Lab Chip* **2015**, *15*, 1153−1159.
(11) Rotem, A.; Ram, O.; Shoresh, N.; Sperling, R. A.; Goren, A.; Weitz, D. A.; Bernstein, B. E. *Nat. Biotechnol.* **2015**, *33*, 1165−1172.
(12) Yuan, H.; Chao, Y.; Li, S.; Tang, M. Y. H.; Huang, Y.; Che, Y.; Wong, A. S. T.; Zhang, T.; Shum, H. C. *Anal. Chem.* **2018**, *90*, 13173−13177.
(13) Mahler, L.; Wink, K.; Beulig, R. J.; Scherlach, K.; Tovar, M.; Zang, E.; Martin, K.; Hertweck, C.; Belder, D.; Roth, M. *Sci. Rep.* **2018**, *8*, 13087.
(14) Eastburn, D. J.; Sciambi, A.; Abate, A. R. *PLoS One* **2013**, *8*, No. e62961.
(15) Lan, F.; Demaree, B.; Ahmed, N.; Abate, A. R. *Nat. Biotechnol.* **2017**, *35*, 640−646.
(16) Qiao, Y.; Zhao, X.; Zhu, J.; Tu, R.; Dong, L.; Wang, L.; Dong, Z.; Wang, Q.; Du, W. *Lab Chip* **2018**, *18*, 190−196.
(17) Li, S.; Zeng, M.; Gaule, T.; McPherson, M. J.; Meldrum, F. C. *Small* **2017**, *13*, 1702154.
(18) Doonan, S. R.; Bailey, R. C. *Anal. Chem.* **2017**, *89*, 4091−4099.
(19) McDonald, J. C.; Duffy, D. C.; Anderson, J. R.; Chiu, D. T.; Wu, H.; Schueller, O. J. A.; Whitesides, G. M. *Electrophoresis* **2000**, *21*, 27−40.
(20) Mazutis, L.; Gilbert, J.; Ung, W. L.; Weitz, D. A.; Griffiths, A. D.; Heyman, J. A. *Nat. Protoc.* **2013**, *8*, 870−891.
(21) Eastburn, D. J.; Sciambi, A.; Abate, A. R. *Anal. Chem.* **2013**, *85*, 8016−8021.
(22) Li, L.; Boedicker, J. Q.; Ismagilov, R. F. *Anal. Chem.* **2007**, *79*, 2756−2761.
(23) Jakiela, S.; Kaminski, T. S.; Cybulski, O.; Weibel, D. B.; Garstecki, P. *Angew. Chem., Int. Ed.* **2013**, *52*, 8908−8911.
(24) Martinez, R.; Jakob, F.; Tu, R.; Siegert, P.; Maurer, K.-H.; Schwaneberg, U. *Biotechnol. Bioeng.* **2013**, *110*, 711−720.
(25) Holstein, J. M.; Gylstorff, C.; Hollfelder, F. *ACS Synth. Biol.* **2021**, *10*, 252−257.
(26) Sjostrom, S. L.; Joensson, H. N.; Svahn, H. A. *Lab Chip* **2013**, *13*, 1754−1761.
(27) Xu, P.; Modavi, C.; Demaree, B.; Twigg, F.; Liang, B.; Sun, C.; Zhang, W.; Abate, A. R. *Nucleic Acids Res.* **2020**, *48*, e48.

https://doi.org/10.1021/acs.analchem.1c02721
Anal. Chem. 2021, 93, 13112−13117